

Electronic Supplementary Information (ESI) for New Journal of Chemistry

New binuclear Ni(II) metallates containing ONS chelators: Synthesis, Characterisation, DNA binding, DNA cleavage, Protein binding, Antioxidant activity, Antimicrobial and *in vitro* Cytotoxicity.

G. Kalaiarasi,^a Ruchi Jain,^b H.Puschman,^c S. Poorna Chandrika,^d K. Preethi^d and R. Prabhakaran.^{a*}

^a Department of Chemistry, Bharathiar University, Coimbatore 641 046, India.

^b Department of Molecular Reproduction, Development and Genetics, Indian Institute of Science, Bangalore 560012, India.

^c Department of Chemistry, Durham University, Durham, DH1 3LE, UK

^d Department of Microbial Biotechnology, Bharathiar University, Coimbatore 641046, India.

Corresponding author Tel.: +91-422-2428319; Fax: +91-422-2422387; E-Mail: rpnchemist@gmail.com (R. Prabhakaran)

Supplementary Information

Experimental procedure

DNA binding study

All of the experiments involving the binding of the complexes with CT DNA were carried out in deionised water with tris(hydroxymethyl)-aminomethane (Tris, 5 mM) and sodium chloride (50 mM) and adjusted to pH 7.2 with hydrochloric acid at room temperature. The concentration of CT-DNA was determined by UV absorbance at 260 nm. Solutions of CT-DNA in Tris-HCl buffer gave a ratio of UV absorbance at 260 and 280 nm, A_{260}/A_{280} , of approximately 1.9, indicating that the DNA was sufficiently free of protein.⁶³ The molar absorption coefficient, ϵ_{260} , was taken as $6600 \text{ M}^{-1} \text{ cm}^{-1}$. Various concentrations of CT-DNA (0–50 μM) was added to the complexes (10 μM dissolved in a DMSO/H₂O mixture, 1 % DMSO in the final solution). While measuring the absorption spectra, an equal amount of DNA was added to both the test solution and the reference solution to eliminate the absorbance of DNA itself. Control experiments with DMSO were performed and no changes in the spectra of CT-DNA were observed. Absorption spectra were recorded after equilibrium at 20° C for 10 min. The intrinsic binding constant K_b was determined by using following equation(1)

$$[\text{DNA}]/[\epsilon_a - \epsilon_f] = [\text{DNA}]/[\epsilon_b - \epsilon_f] + 1/K_b[\epsilon_b - \epsilon_f] \quad (1)$$

The absorption coefficients ϵ_a , ϵ_f and ϵ_b correspond to $A_{\text{obsd}} / [\text{DNA}]$, the extinction coefficient for the free complex and the extinction coefficient for the complex in the fully bound form respectively. The slope and the intercept of the linear fit of the plot of $[\text{DNA}]/[\epsilon_a - \epsilon_f]$ versus $[\text{DNA}]$ give $1/[\epsilon_a - \epsilon_f]$ and $1/K_b[\epsilon_b - \epsilon_f]$, respectively. The intrinsic binding constant K_b can be obtained from the ratio of the slope to the intercept.⁴⁵ In order to find out the mode of attachment of CT DNA to the complexes (**1-4**), fluorescence quenching experiments of EB-DNA were carried out by adding our complexes to the Tris-HCl buffer of EB-DNA. The change in the fluorescence intensity was recorded. Before measurements, the system was shaken well and incubated at room temperature for 5 min. The emission was recorded at 530–750 nm.

Bovine serum albumin binding study

Bovine Serum Albumin (BSA) was purchased from Hi Media, India. BSA solution (10 μM) was prepared in phosphate buffer of pH 7.2 and stored in the dark at 4 $^\circ\text{C}$ for use. The protein binding study was performed by tryptophan fluorescence quenching experiments using bovine serum albumin (BSA, 10 μM) as the substrate in phosphate buffer (pH = 7.2). Quenching of the emission intensity of tryptophan residues of BSA at 346 nm (excitation wavelength at 280 nm) was monitored using complex as quenchers with increasing complex concentration (10-100 μM). Synchronous fluorescence spectra of BSA with various concentrations of the complexes were obtained from 300 to 400 nm when $\Delta\lambda = 60$ nm and from 290 to 500 nm when $\Delta\lambda = 15$ nm. The excitation and emission slit widths were 5 and 6 nm, respectively. For synchronous fluorescence spectra, the same concentrations of BSA and the compounds were also used and the spectra were measured at two different $\Delta\lambda$ values (difference between the excitation and emission wavelengths of BSA), such as 15 and 60 nm. Fluorescence and synchronous measurements were performed using a 1 cm quartz cell on a JASCO FP 6600 spectrofluorimeter.

Table S1. Analytical and IR data of the ligands and new nickel(II) complexes

Compound	Elemental analyses Calc. (Found) %				IR spectral data (cm ⁻¹)				
	C	H	N	S	ν_{OH}	$\nu_{C=N}$	ν_{C-O}	$\nu_{C=S}$	ν_{C-S}
[H ₂ -Msal-tsc] (H ₂ L ¹)	47.98 (47.76)	4.92 (5.00)	18.65 (18.67)	14.23 (14.20)	3458	1593	1272	771	-
[H ₂ -Msal-mtsc](H ₂ L ²)	50.19 (50.15)	5.47 (5.40)	17.56 (17.49)	13.40 (13.31)	3338	1554	1276	780	-
[H ₂ -Msal-etsc] (H ₂ L ³)	55.21 (55.15)	6.31 (6.27)	16.58 (16.50)	12.65 (12.59)	3310	1536	1276	795	-
[H ₂ -Msal-ptsc] (H ₂ L ⁴)	59.81 (59.65)	5.12 (4.99)	13.95 (13.78)	10.64 (10.43)	3339	1589	1273	782	-
[Ni ₂ (Msal-tsc) ₂ (μ -dppe)]	54.92 (54.89)	4.39 (4.34)	8.73 (8.68)	6.66 (6.60)	-	1627	1311	-	711
[Ni ₂ (Msal-mtsc) ₂ (μ -dppe)]	55.79 (55.73)	4.68 (4.64)	8.49 (8.46)	6.48 (6.45)	-	1638	1317	-	743
[Ni ₂ (Msal-etsc) ₂ (μ -dppe)]	56.61 (56.57)	4.95 (4.90)	8.25 (8.22)	6.30 (6.28)	-	1635	1363	-	734
[Ni ₂ (Msal-ptsc) ₂ (μ -dppe)]	60.35 (60.31)	4.52 (4.48)	7.54 (7.49)	5.75 (5.71)	-	1638	1313	-	727

Table S2. Electronic spectral data of the new nickel(II) Complexes

Complex	λ_{max} (ϵ) (nm) (dm ³ mol ⁻¹ cm ⁻¹)
[Ni ₂ (Msal-tsc) ₂ (μ -dppe)]	259 (55990) (intra-ligand transition) 307(23373) and 368(18551) (LMCT s→d) 409 (8281) (MLCT)
[Ni ₂ (Msal-mtsc) ₂ (μ -dppe)]	244 (46203) (intra-ligand transition) 361 (11994) (LMCT s→d) 409 (6897) (MLCT)
[Ni ₂ (Msal-etsc) ₂ (μ -dppe)]	256 (97141) (intra-ligand transition) 306 (42441) and 361 (23658) (LMCT s→d) 416 (12535) (MLCT)
[Ni ₂ (Msal-ptsc) ₂ (μ -dppe)]	281 (86490) (intra-ligand transition) 370 (36594) (LMCT s→d) 426 (21822) (MLCT)

Table S3: The radical scavenging activity of ligands, 1,2-bis(diphenylphosphino)ethane (dppe), NiCl₂.6H₂O and new Ni(II) complexes

Compounds	IC ₅₀ values (μM)	
	DPPH [•]	O ₂ ^{-•}
Standard	327.16±5.68	288.55±1.14
H ₂ L ¹	248.97±2.44	225.86±2.00
H ₂ L ²	228.83±2.29	179.58±1.41
H ₂ L ³	213.84±3.76	141.72±1.45
H ₂ L ⁴	215.65±4.12	170.29±1.24
NiCl ₂ .6H ₂ O	237.68±7.40	195.99±1.30
dppe	133.61±0.51	108.29±0.29
Complex 1	28.95±0.13	31.45±0.15
Complex 2	24.79±0.21	30.89±0.23
Complex 3	15.58±0.26	25.07±0.10
Complex 4	29.26±0.10	31.50±0.09

Table S4: The IC₅₀ values for the human breast cancer cell line MCF-7 and human cervical cancer cell line HeLa with the ligands, bis(diphenylphosphino)ethane (dppe) and NiCl₂.6H₂O for 48 h

Compounds	IC ₅₀ values (μM)	
	MCF-7	HeLa
Cisplatin	23.70±0.07	23.00±0.01
H ₂ L ¹	13.65±0.07	12.53±0.10
H ₂ L ²	18.23±0.05	19.74±0.09
H ₂ L ³	9.07±0.06	12.94±0.12
H ₂ L ⁴	16.70±0.09	18.70±0.10
NiCl ₂ .6H ₂ O	41.74±0.05	42.47±0.04
dppe	31.19±0.09	35.27±0.03

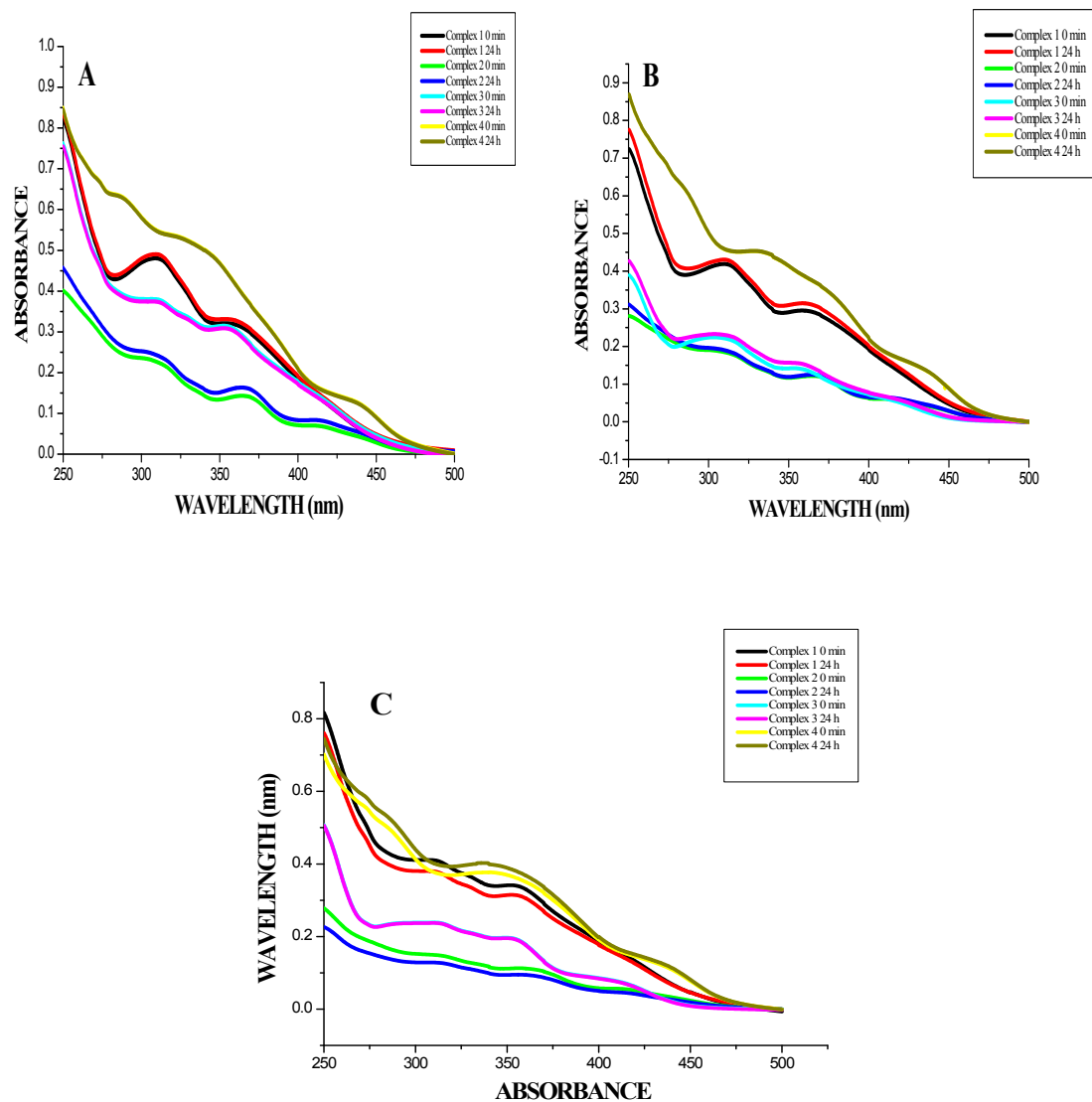


Fig. S1. Stability studies of the complexes using UV-Vis absorption spectroscopic technique. A) absorption spectra complexes in 1% aqueous DMSO; B) absorption spectra complexes in 99: 1 phosphate buffer: DMSO; B) absorption spectra complexes in 99: 1 tris HCl buffer : DMSO

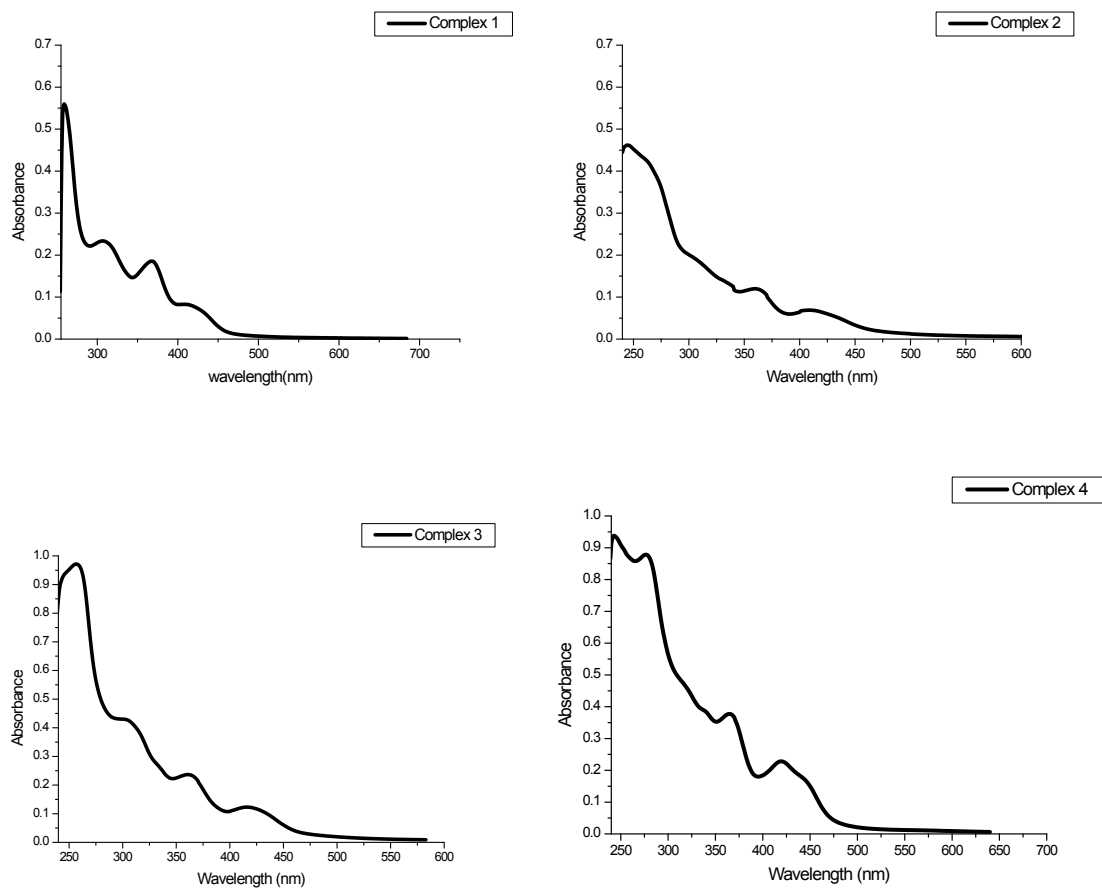


Fig. S2. Electronic spectra of the complexes (1-4).

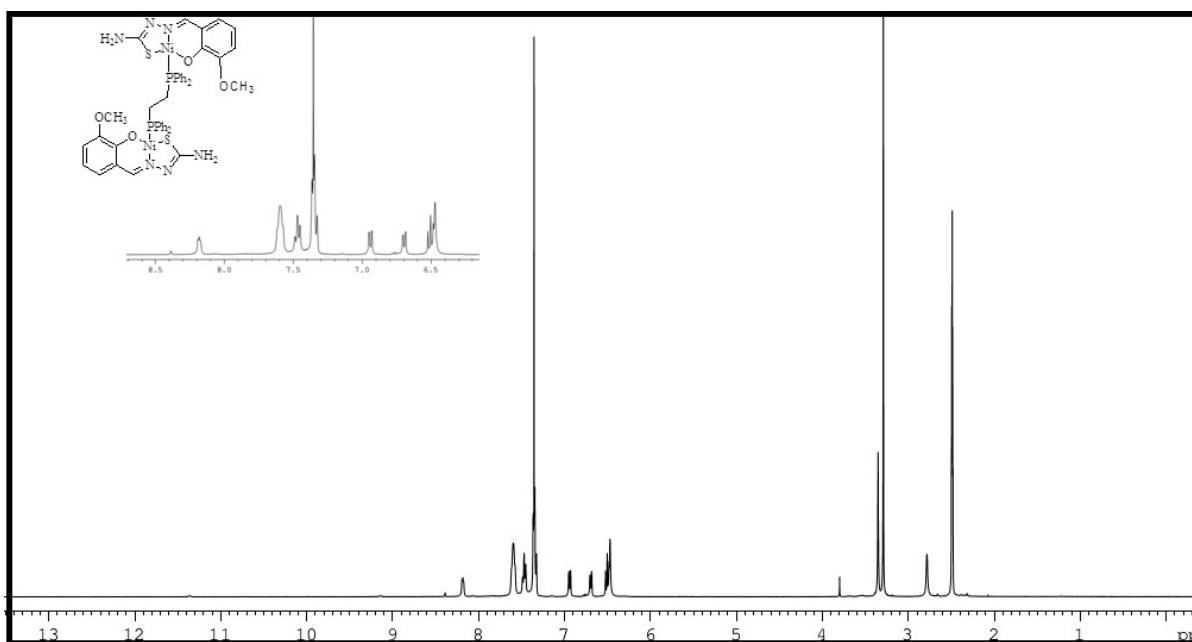


Fig. S3 $^1\text{H-NMR}$ spectrum of $[\text{Ni}_2(\text{Msal-tsc})_2(\mu\text{-dppe})]$ (1)

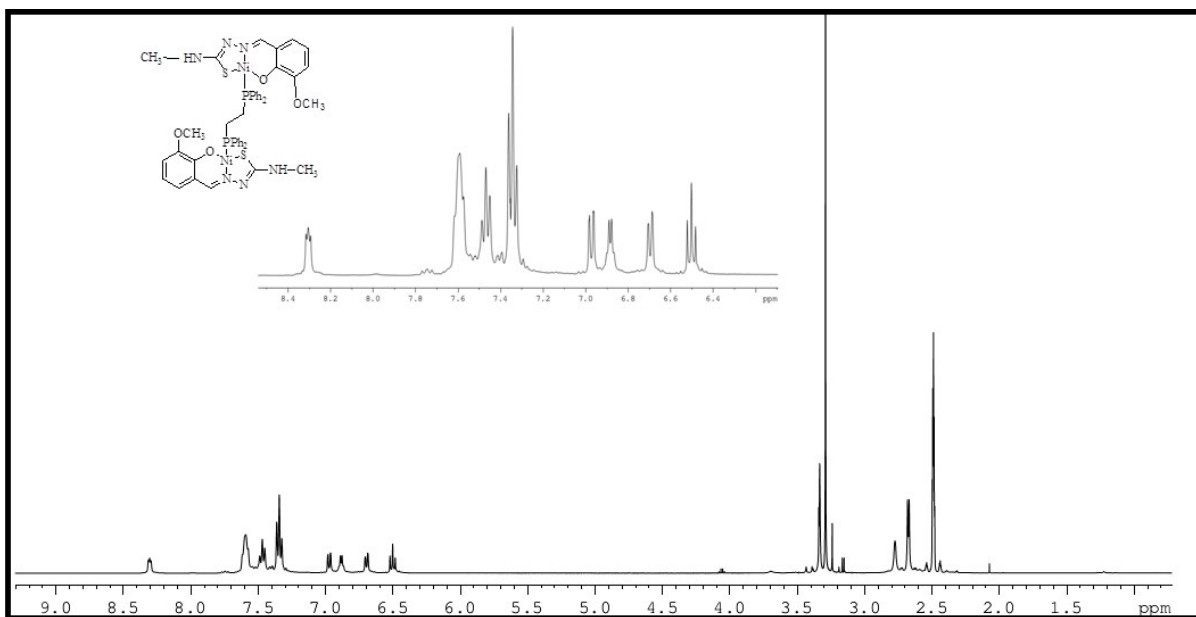


Fig. S4. $^1\text{H-NMR}$ spectrum of $[\text{Ni}_2(\text{Msal-mtsc})_2(\mu\text{-dppe})]$ (2)

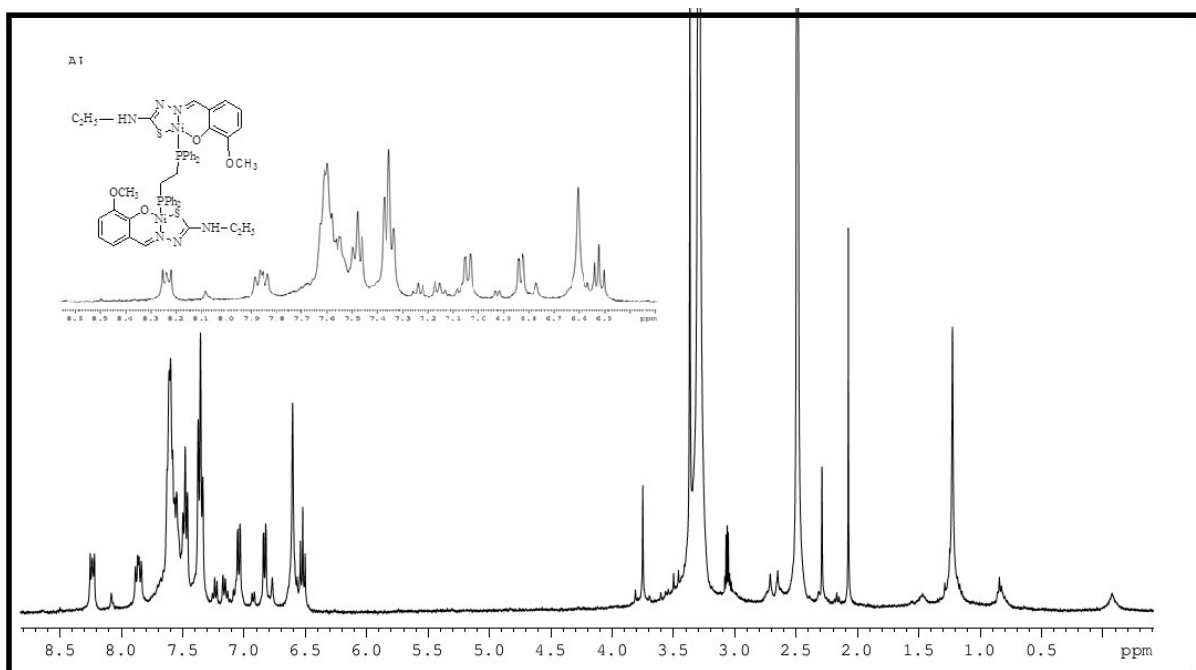


Fig. S5. $^1\text{H-NMR}$ spectrum of $[\text{Ni}_2(\text{Msal-etsc})_2(\mu\text{-dppe})]$ (3)

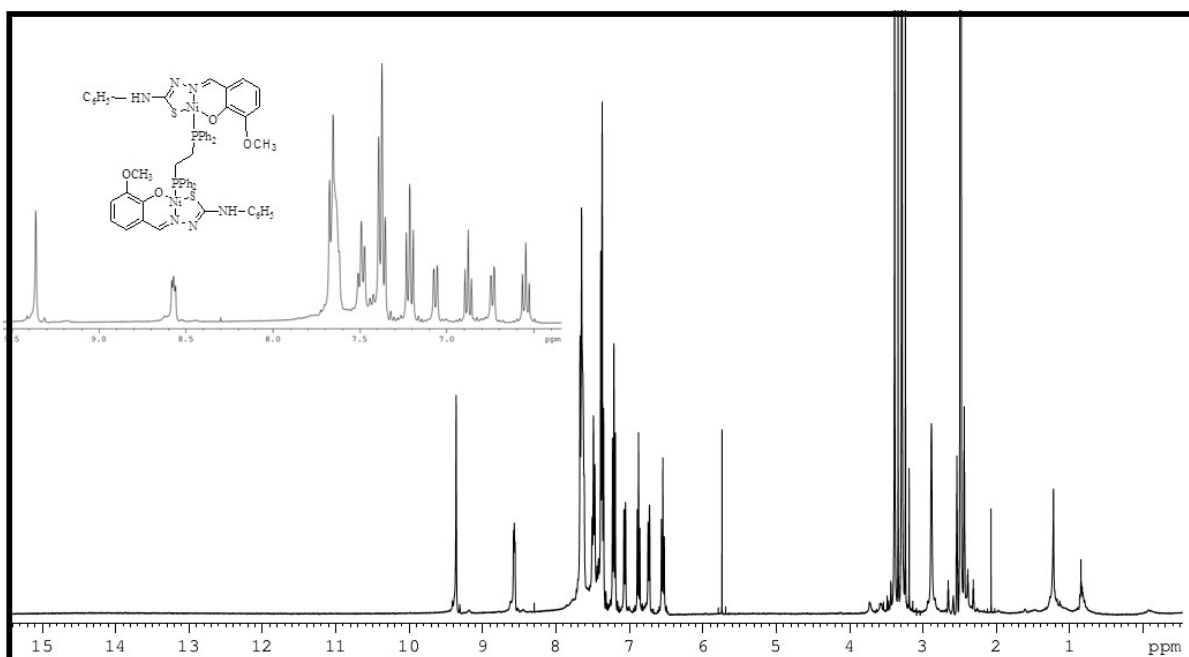


Fig. S6. ^1H -NMR spectrum of $[\text{Ni}_2(\text{Msal-ptsc})_2(\mu\text{-dppe})]$ (**4**)

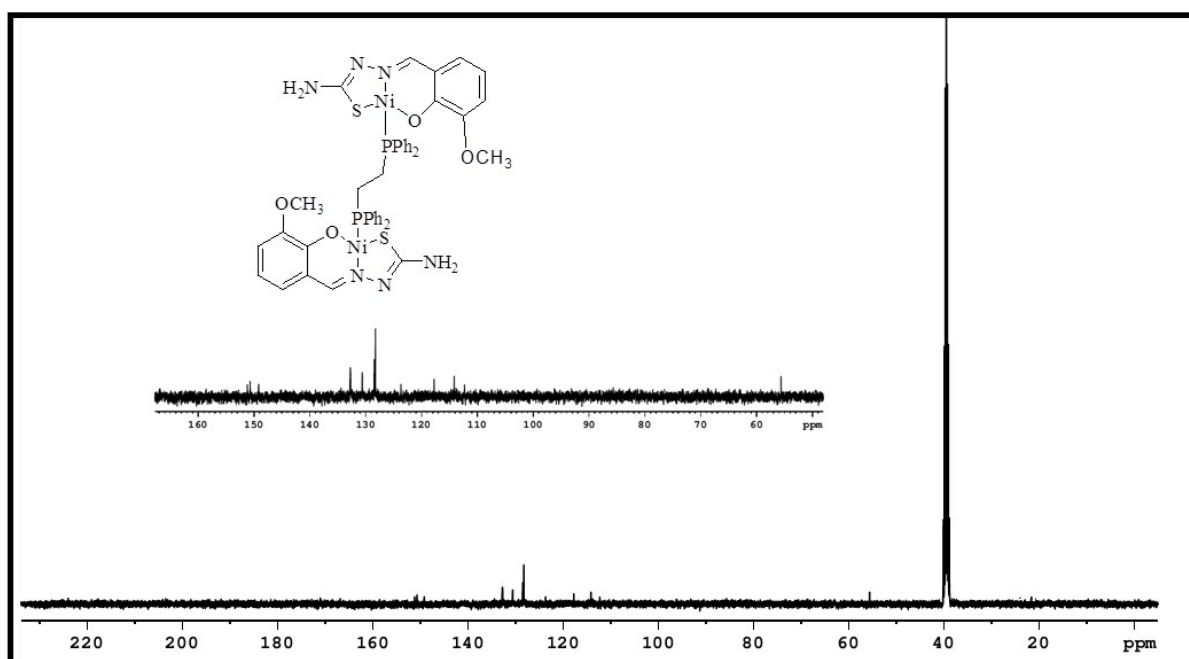


Fig. S7. ^{13}C -NMR spectrum of $[\text{Ni}_2(\text{Msal-tsc})_2(\mu\text{-dppe})]$ (**1**)

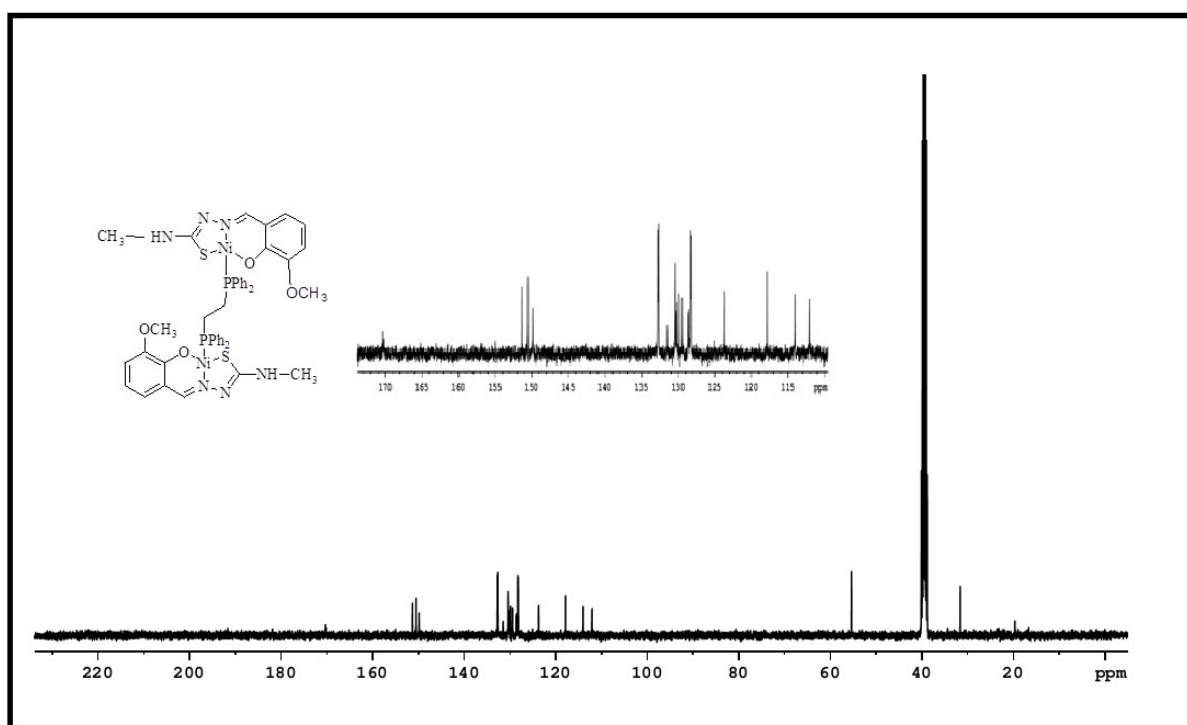


Fig. S8. ^{13}C -NMR spectrum of $[\text{Ni}_2(\text{Msal-mtsc})_2(\mu\text{-dppe})]$ (**2**)

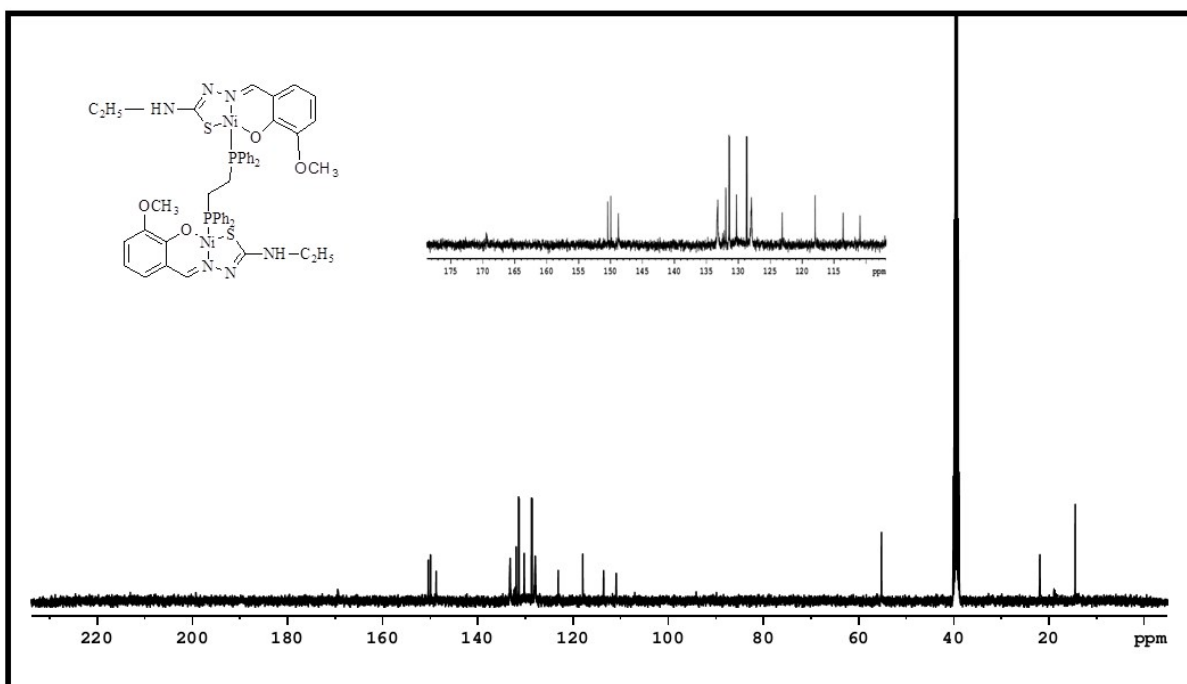


Fig. S9. ^{13}C -NMR spectrum of $[\text{Ni}_2(\text{Msal-etsc})_2(\mu\text{-dppe})]$ (**3**)

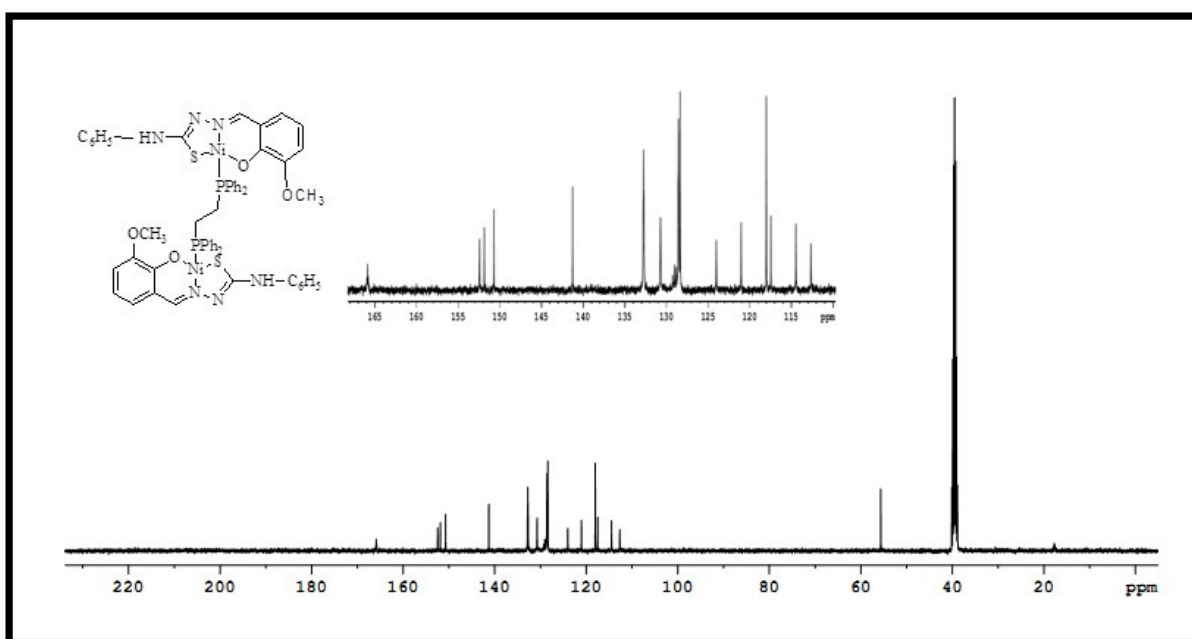


Fig. S10. $^{13}\text{C-NMR}$ spectrum of $[\text{Ni}_2(\text{Msal-ptsc})_2(\mu\text{-dppe})]$ (4)

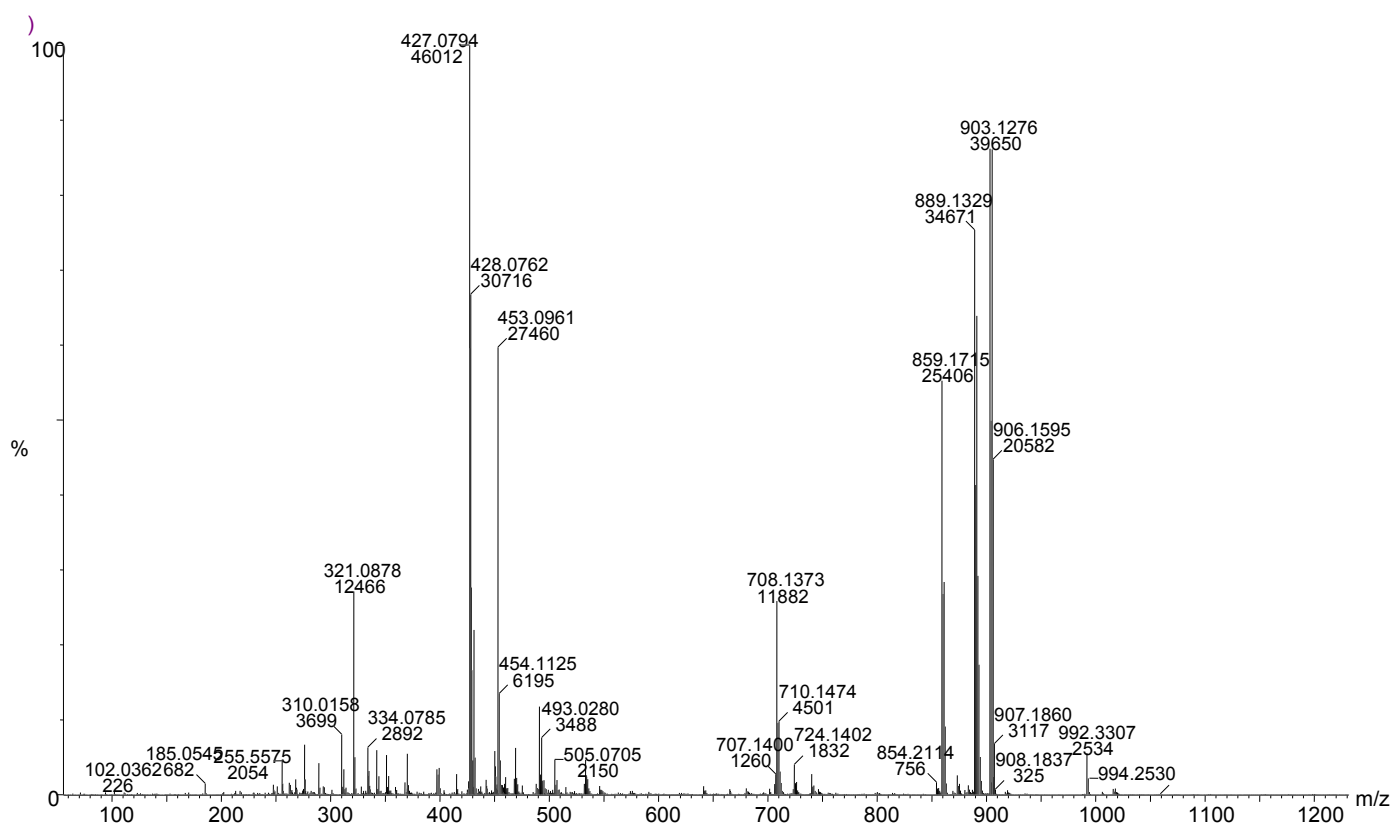


Fig. S11. ESI-MS spectrum of $[\text{Ni}_2(\text{Msal-mtsc})_2(\mu\text{-dppe})]$ (2)

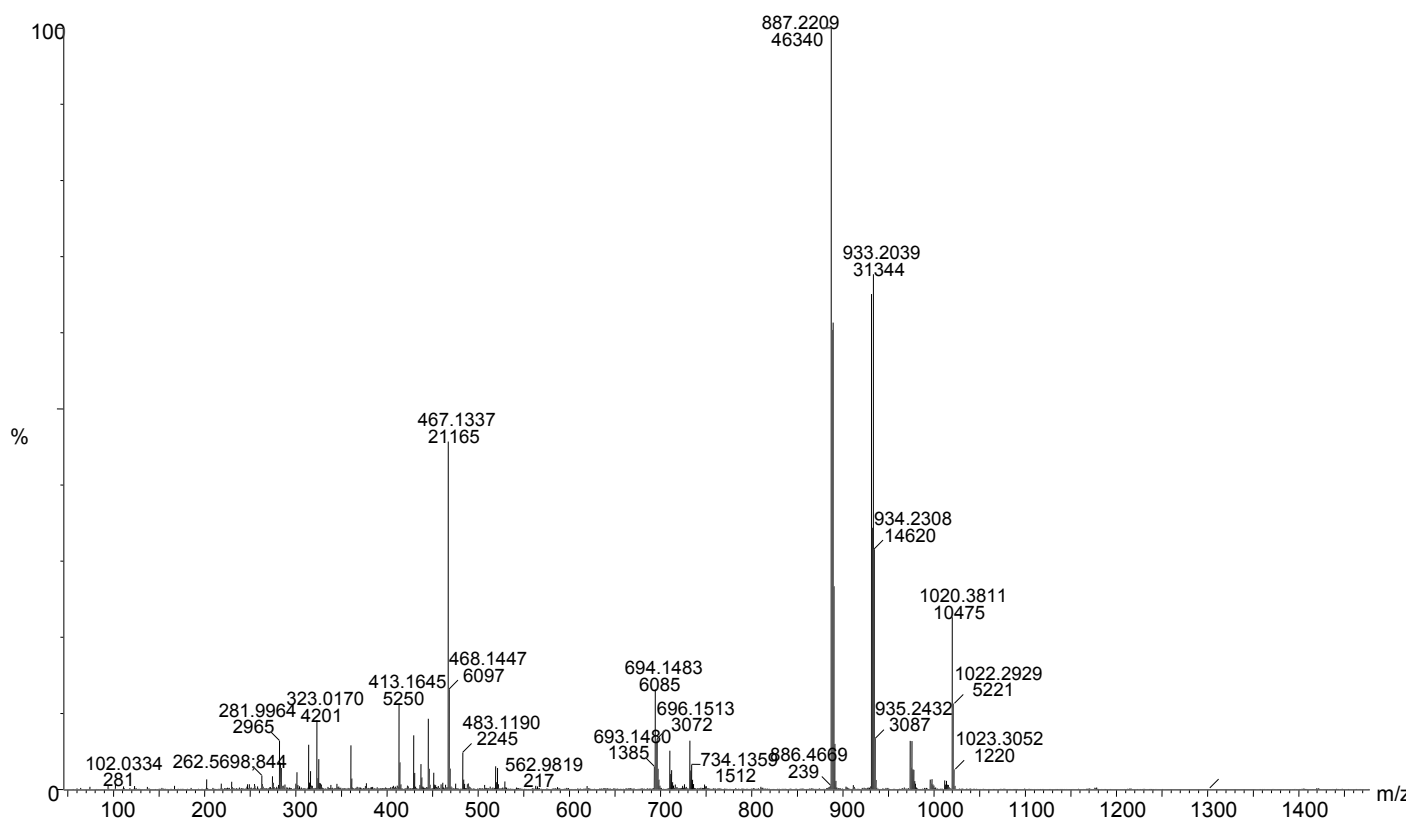


Fig. S12. ESI-MS spectrum of $[\text{Ni}_2(\text{Msal-etsc})_2(\mu\text{-dppe})]$ (**3**)

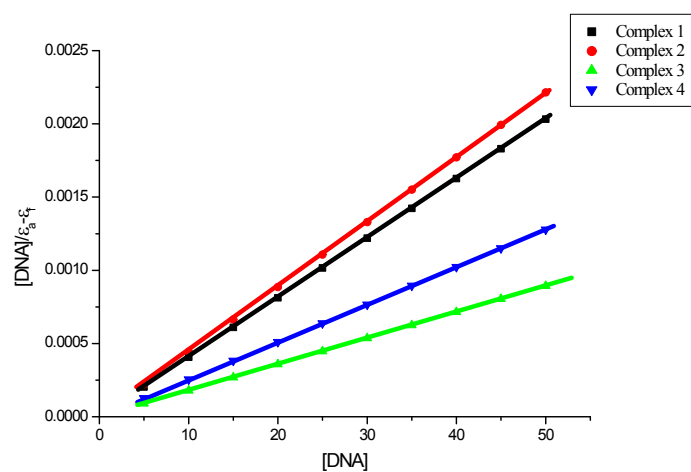


Fig. S13. Binding isotherms of the complexes **1-4** with CT-DNA.

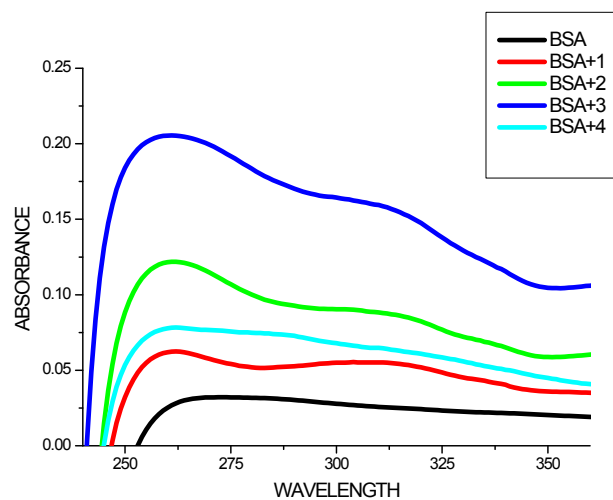


Fig. S14. Absorption spectra of absence and presence of complexes(1-4) with BSA (1×10^{-5} M)

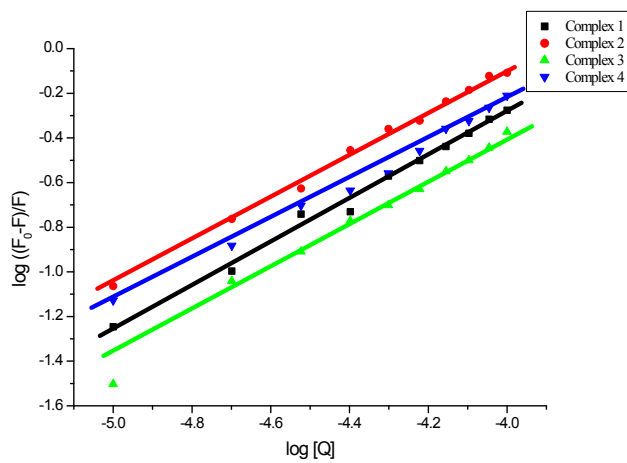


Fig. S15. Scatchard plot of the fluorescence titration of the complexes (1-4) (10-100 μ M) with BSA (10 μ M).

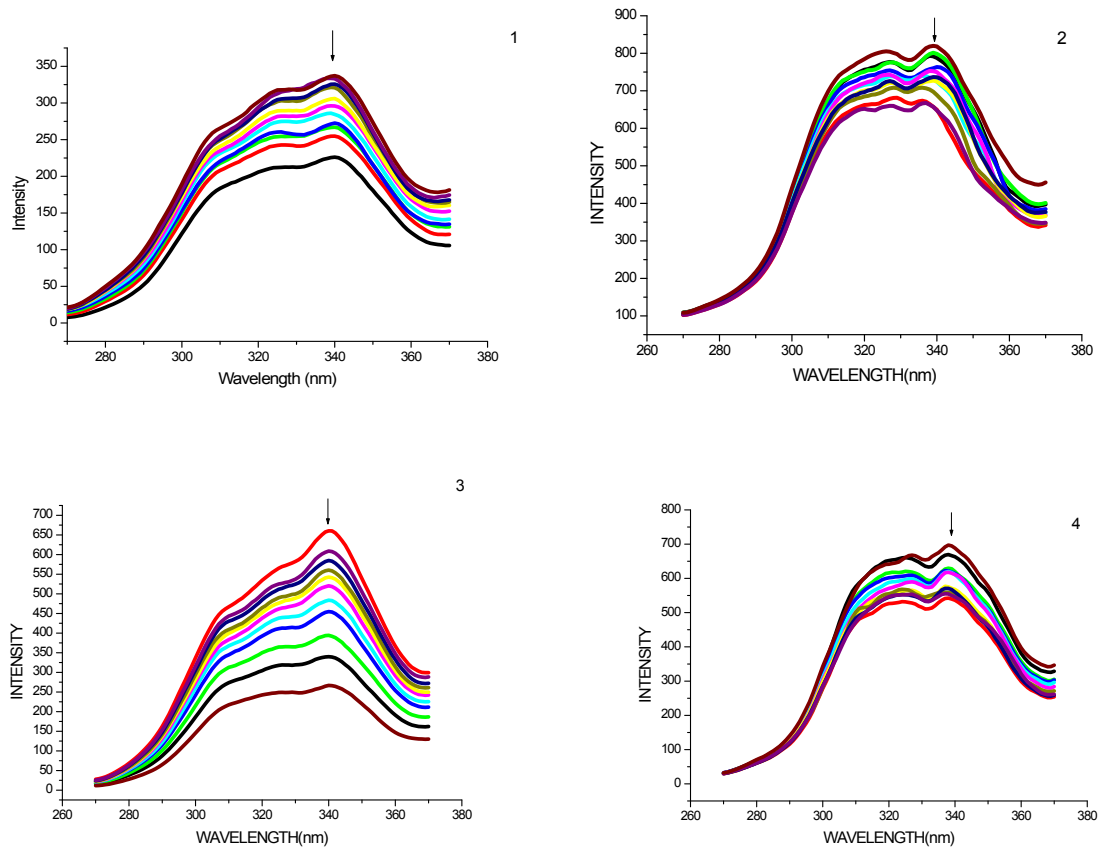


Fig. S16. Synchronous spectra of BSA (10 μM) in the presence of increasing amounts of complexes **1-4** (10–100 μM) for a wavelength difference of $\Delta\lambda=15$ nm. The arrow shows the emission intensity changes upon increasing concentration of complex

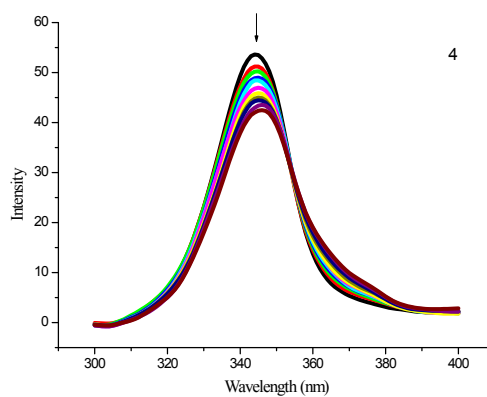
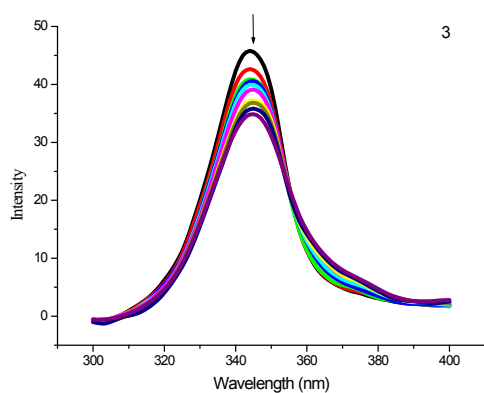
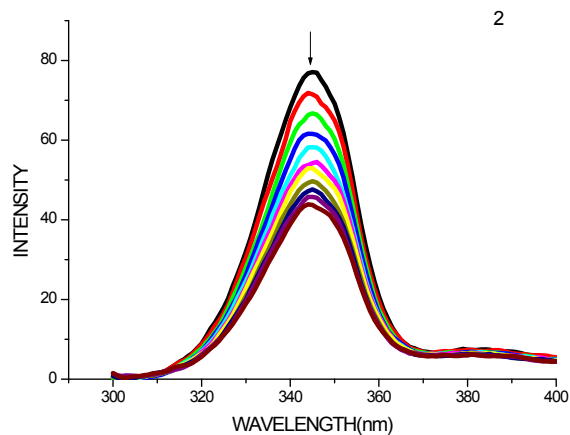
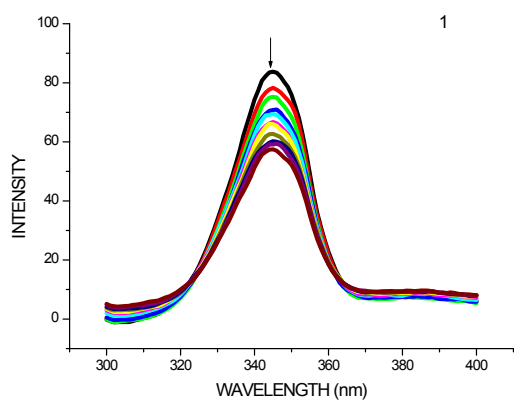


Fig. S17. Synchronous spectra of BSA (10 μM) in the presence of increasing amounts of complexes **1-4** (10–100 μM) for a wavelength difference of $\Delta\lambda=60$ nm. The arrow shows the emission intensity changes upon increasing concentration of complex

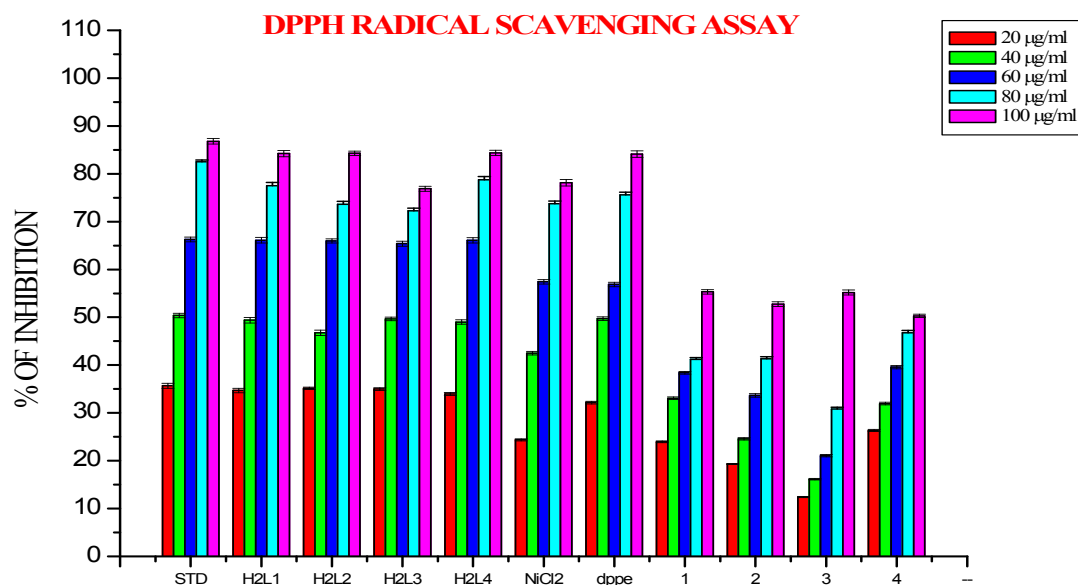


Fig. S18. DPPH scavenging activity of ligands, 1,2-bis(diphenylphosphino)ethane (dppe), NiCl₂.6H₂O and new Ni(II) complexes. Error bars represent the standard deviation of the mean(n=3)

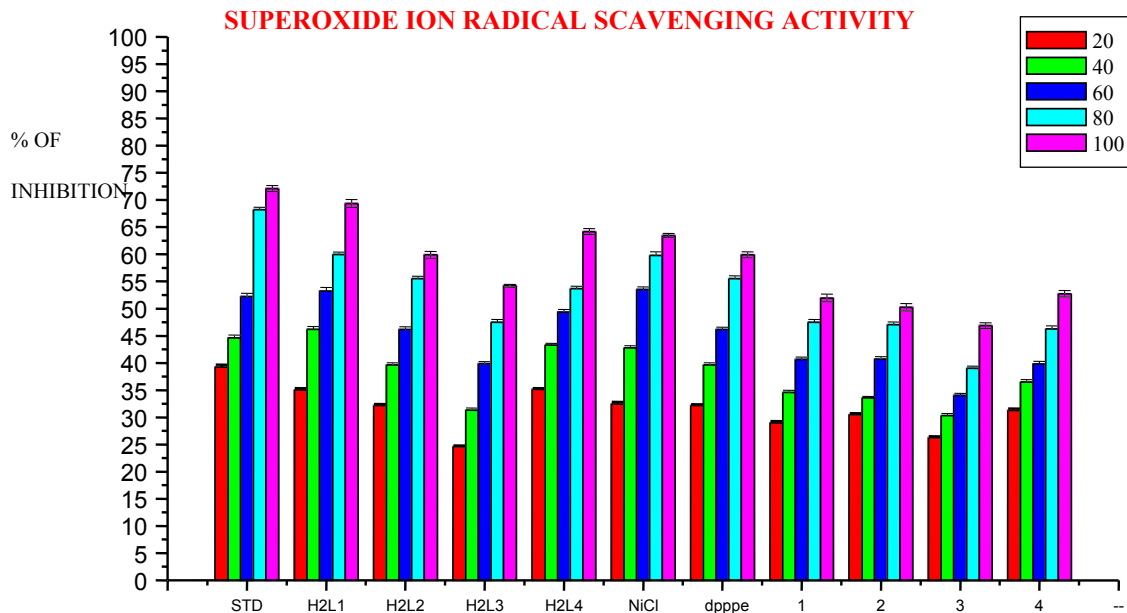


Fig. S19. Superoxide scavenging activity of ligands, 1,2-bis(diphenylphosphino)ethane (dppe), NiCl₂.6H₂O and new Ni(II) complexes. Error bars represent the standard deviation of the mean (n=3)

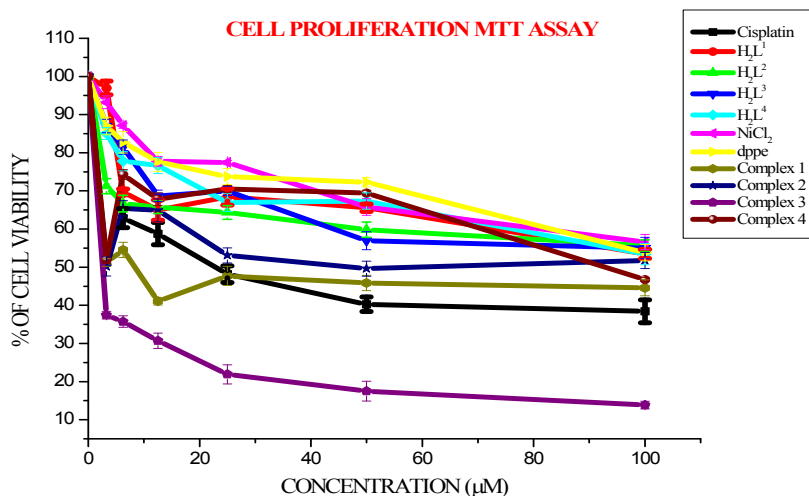


Fig. S20. The newly synthesized nickel complexes (**1-4**) inhibit MCF-7 cell proliferation in a dose dependent manner. MCF-7 cells were treated with different concentrations of compounds for 24 h, the cell viability was determined and the results were expressed as percentage cell viability with control. Results shown are mean, which are three separate experiments performed in triplicate.

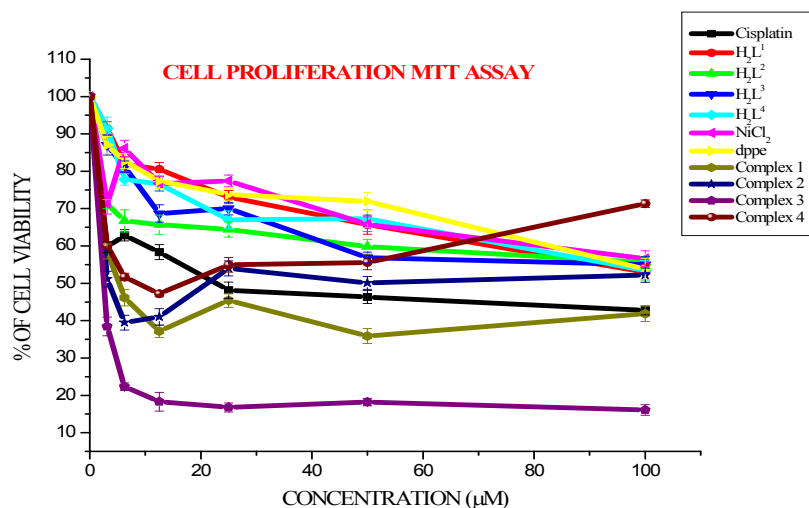


Fig. S21. The newly synthesized nickel complexes (**1-4**) inhibit HeLa cell proliferation in a dose dependent manner. HeLa cells were treated with different concentrations of compounds for 24 h, the cell viability was determined and the results were expressed as percentage cell viability with control. Results shown are mean, which are three separate experiments performed in triplicate.

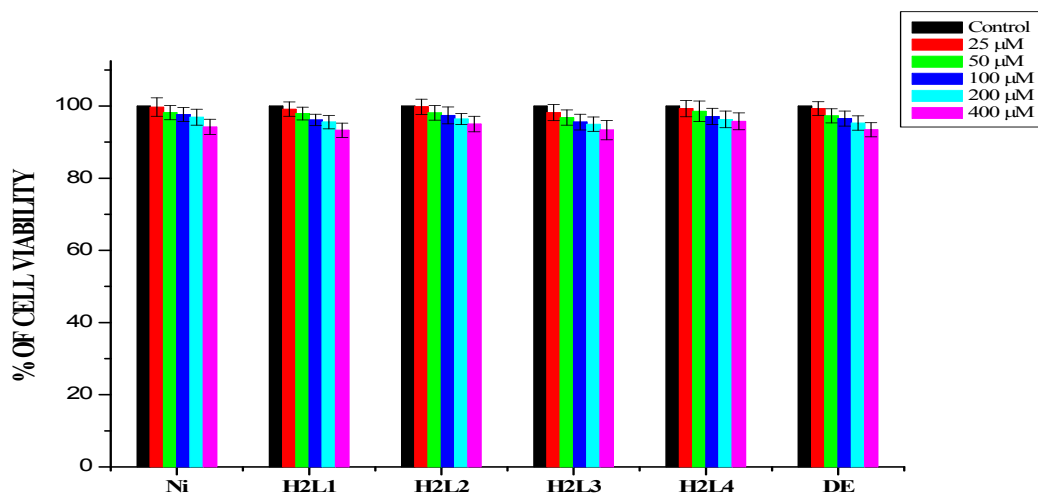


Fig. S22. The compounds inhibit HaCaT cell proliferation in a dose dependent manner. HaCaT cells were treated with different concentrations of compounds for 24 h, the cell viability was determined and the results were expressed as percentage cell viability with control. Results shown are mean, which are three separate experiments performed in triplicate.

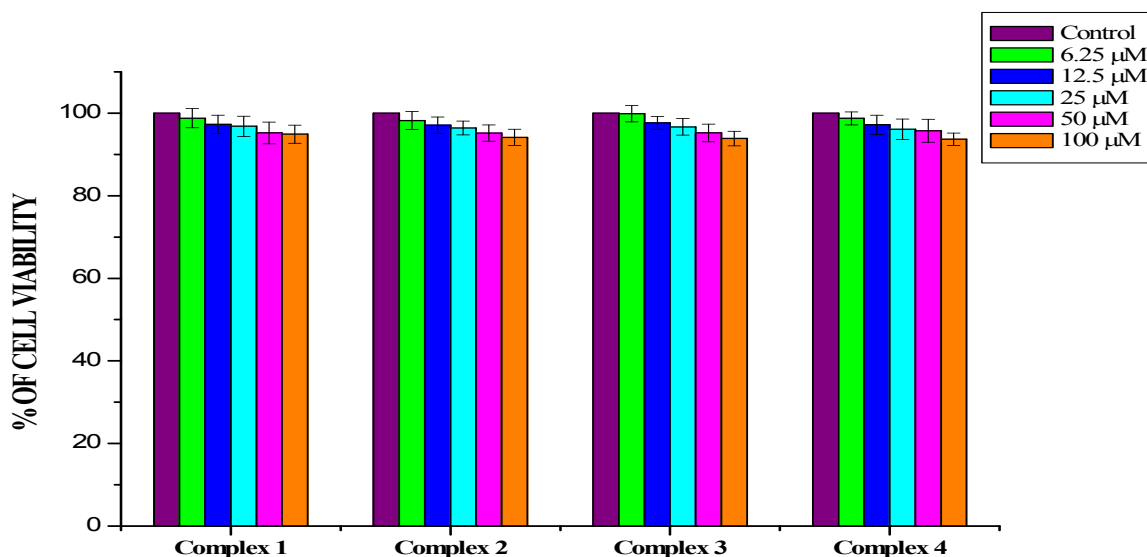


Fig. S23. The newly synthesized nickel complexes (1-4) inhibit HaCaT cell proliferation in a dose dependent manner. HaCaT cells were treated with different concentrations of compounds for 24 h, the cell viability was determined and the results were expressed as percentage cell viability with control. Results shown are mean, which are three separate experiments performed in triplicate.

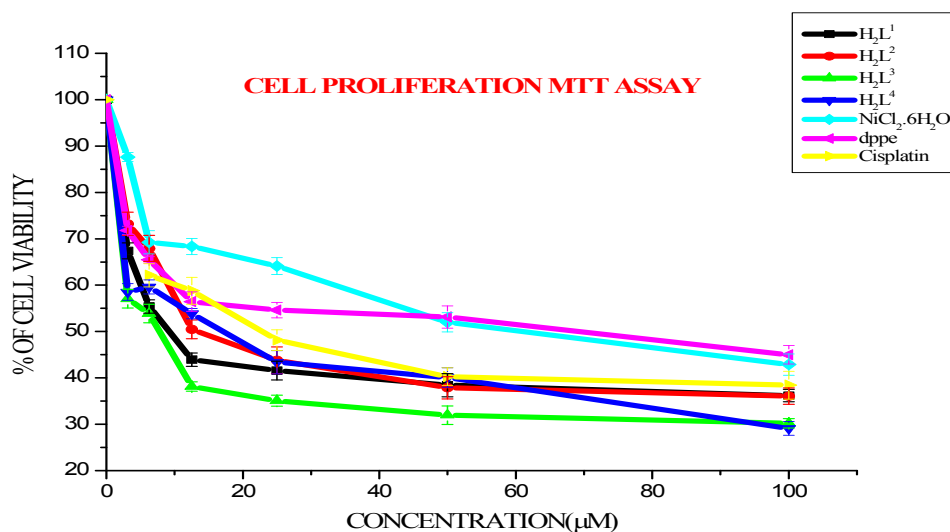


Fig. S24. The ligands H_2L^{1-4} , $NiCl_2 \cdot 6H_2O$, 1,2-bis(diphenylphosphino)ethane inhibit MCF-7 cell proliferation in a dose dependent manner. MCF-7 cells were treated with different concentrations of these compounds for 48 h, the cell viability was determined and the results were expressed as percentage cell viability with control. Results shown are mean \pm SD, which are three separate experiments performed in triplicate

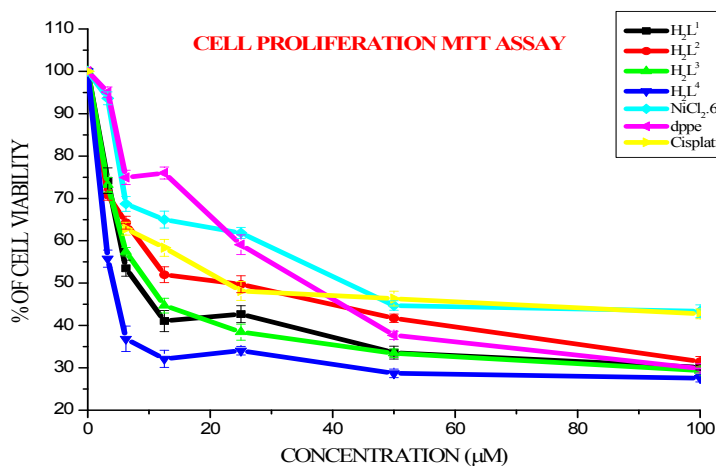


Fig. S25. The ligands H_2L^{1-4} , $NiCl_2 \cdot 6H_2O$ and 1,2-bis(diphenylphosphino)ethane inhibit HeLa cell proliferation in a dose dependent manner. HeLa cells were treated with different concentrations of these compounds for 48 h, the cell viability was determined and the results were expressed as percentage cell viability with control. Results shown are mean \pm SD, which are three separate experiments performed in triplicate

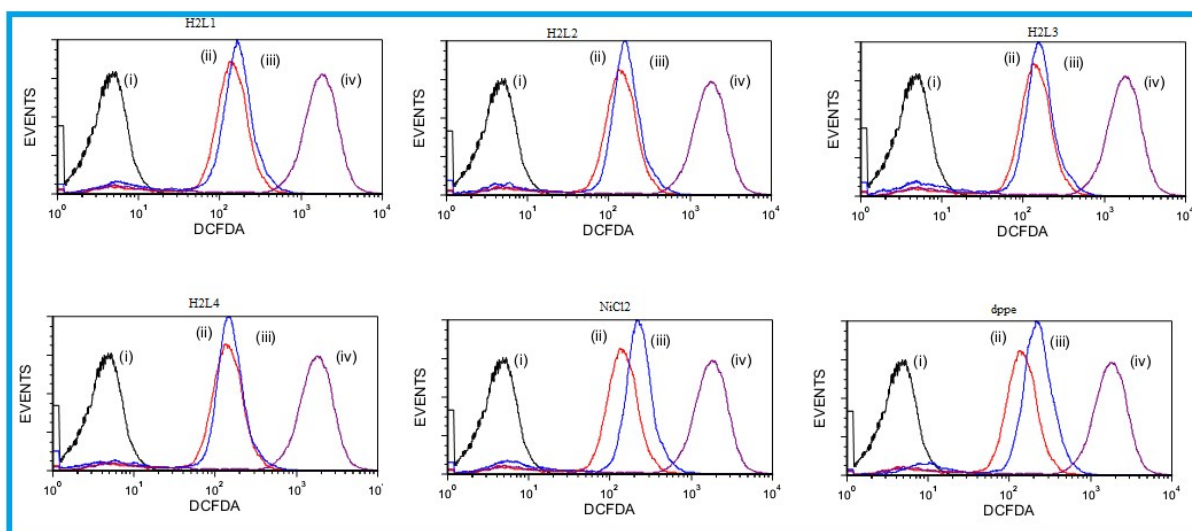


Fig. S26. Flow cytometric analysis (FACS) for ROS generation by ligands, NiCl₂ and dppe were performed using the DCFDA dye. (i) the fluorescence of cells alone, (ii): the fluorescence of cells + DCFDA, (iii) the fluorescence of cells + DCFDA + IC₅₀ concentration of compounds (iv) fluorescence of cells + DCFDA + control